

Interferometers

13.1 Introduction

The discussion of modules and computerization in previous chapters gives us the means to consider empirically useful quantized detector networks (QDN). In this chapter we shall focus on a particular class of network known as *interferometers*.

Interferometers play a crucial role in quantum mechanics (QM) because they demonstrate the “paradox” of wave–particle duality in a direct way. On the one hand, discrete signals are detected by the observer and those signals are usually interpreted as particles or quanta. On the other hand, the observed frequencies built up over many runs show effects interpreted as due to the interference of waves.

In the previous chapter, we used computer algebra (CA) to discuss the Wolaston interferometer (WI), a relatively simple interferometer. We shall use the same approach in the following discussion of the Mach–Zehnder interferometer (MZI), apparatus that allows the observer to investigate optical transmission through various materials.

13.2 The Mach–Zehnder Interferometer

The basic structure of an MZI is given in Figure 13.1. A source S of light sends a monochromatic, unpolarized beam 1_0 into one input channel of beam splitter B^1 . Output channel 1_1 is deflected by mirror M^1 onto a module labeled ϕ that contains some medium under investigation, such as a crystal or liquid. The net effect is to create a phase change in that deflected beam by an amount ϕ , and then that modified beam, 1_2 , is passed into beam splitter B^2 . The second output channel, 2_1 , from B^1 , meanwhile, is deflected by mirror M^2 into beam splitter B^2 . The two deflected beams, 1_2 and 2_2 , that pass into B^2 interfere and are finally monitored by detectors 1_3 and 2_3 .

Our analysis of the MZI follows the CA approach used for the WI in the previous chapter.

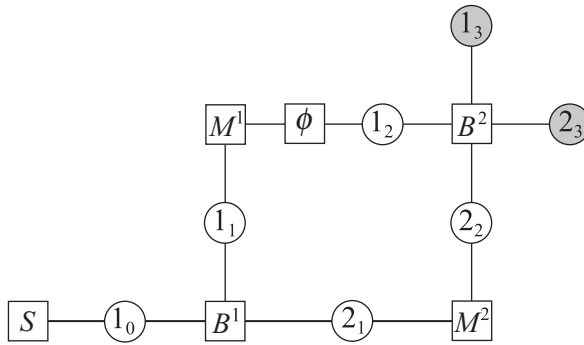


Figure 13.1. The Mach–Zehnder interferometer: S is a source of monochromatic, unpolarized light, B^1 and B^2 are beam splitters, M^1 and M^2 are mirrors, and ϕ contains a medium that changes the phase of the light by ϕ .

Parameters

For this experiment, the number of stages N is $N = 3$. From Figure 13.1, the rank at each stage is seen to be $r_0 = 1, r_1 = r_2 = r_3 = 2$. Since polarization is not a factor in this version of the experiment, we take the dimensions of the internal (photonic) space at the four stages to be given by $d_0 = d_1 = d_2 = d_3 = 1$.

The Initial State

Since we are not interested here with polarization, the initial total state $|\Psi_0\rangle$ is given by $|\Psi_0\rangle \equiv |s_0\rangle \otimes \widehat{\mathbf{A}}_0^1 \mathbf{0}_0 = |s_0\rangle \otimes \mathbf{1}_0$, where $|s_0\rangle$ is a normalized photon state.

From Figure 13.1 and the known properties of the modules, we write

Stage Σ_0 to Stage Σ_1

$$\begin{aligned}
 U_{1,0} \left\{ |s_0\rangle \otimes \widehat{\mathbf{A}}_0^1 \mathbf{0}_0 \right\} &= t^1 |s_1\rangle \otimes \widehat{\mathbf{A}}_1^2 \mathbf{0}_1 + ir^1 |s_1\rangle \otimes \widehat{\mathbf{A}}_1^1 \mathbf{0}_1 \\
 &\equiv |s_1\rangle \otimes (t^1 \mathbf{2}_1 + ir^1 \mathbf{1}_1).
 \end{aligned}
 \tag{13.1}$$

Stage Σ_1 to Stage Σ_2

$$\begin{aligned}
 U_{2,1} \left\{ |s_1\rangle \otimes \widehat{\mathbf{A}}_1^1 \mathbf{0}_1 \right\} &= e^{i\phi} |s_2\rangle \otimes \widehat{\mathbf{A}}_2^1 \mathbf{0}_2 \equiv e^{i\phi} |s_2\rangle \otimes \mathbf{1}_2, \\
 U_{2,1} \left\{ |s_1\rangle \otimes \widehat{\mathbf{A}}_1^2 \mathbf{0}_1 \right\} &= |s_2\rangle \otimes \widehat{\mathbf{A}}_2^2 \mathbf{0}_2 \equiv |s_2\rangle \otimes \mathbf{2}_2.
 \end{aligned}
 \tag{13.2}$$

Stage Σ_2 to Stage Σ_3

$$\begin{aligned}
 U_{3,2} \left\{ |s_2\rangle \otimes \widehat{\mathbf{A}}_2^1 \mathbf{0}_2 \right\} &= t^2 |s_3\rangle \otimes \widehat{\mathbf{A}}_3^2 \mathbf{0}_3 + ir^2 |s_3\rangle \otimes \widehat{\mathbf{A}}_3^1 \mathbf{0}_3 \equiv |s_3\rangle \otimes (t^2 \mathbf{2}_3 + ir^2 \mathbf{1}_3), \\
 U_{3,2} \left\{ |s_2\rangle \otimes \widehat{\mathbf{A}}_2^2 \mathbf{0}_2 \right\} &= ir^2 |s_3\rangle \otimes \widehat{\mathbf{A}}_3^2 \mathbf{0}_3 + t |s_3\rangle \otimes \widehat{\mathbf{A}}_3^1 \mathbf{0}_3 \equiv |s_3\rangle \otimes (ir^2 \mathbf{2}_3 + t \mathbf{1}_3).
 \end{aligned}
 \tag{13.3}$$

Here we have ignored any phase changes at the mirrors and characterized each beam splitter separately. In the above, all superscripts are labels, not powers.

This is all the input information required for our CA program MAIN, as discussed in the previous chapter. The nonzero conditional outcome probabilities are found to be

$$\begin{aligned}\Pr(\widehat{A}_3^1 \mathbf{0}_3 | \Psi_0) &= -2r^1 r^2 t^1 t^2 \cos(\phi) + (r^1 r^2)^2 + (t^1 t^2)^2, \\ \Pr(\widehat{A}_3^2 \mathbf{0}_3 | \Psi_0) &= +2r^1 r^2 t^1 t^2 \cos(\phi) + (r^1 t^2)^2 + (t^1 r^2)^2.\end{aligned}\quad (13.4)$$

These sum up to unity as required, given that $(t^i)^2 + (r^i)^2 = 1$, for $i = 1, 2$.

The significance here is that the outcome probabilities are affected by the phase change module. By altering the path length in that module, and other parameters such as temperature and density of the medium in that module, significant information about that medium can be extracted.

13.3 Brandt's Network

The next example is a quantum optics network discussed by Brandt (Brandt, 1999) in terms of conventional positive operator-valued measure operators (POVMs) and shown in Figure 13.2. A source S prepares a monochromatic unpolarized beam of light 1_0 that is split by Wollaston prism W into two orthogonally polarized components 1_1 and 2_1 . One component 1_1 is then passed into beam splitter B^1 and thereby split into two components 1_2 and 2_2 with no change in polarization. Component 1_2 is subsequently observed at detector 1_3 , while component 2_2 is passed into beam splitter B^2 . Meanwhile, component 2_1 emerging from the Wollaston prism W has its polarization turned by $\pi/2$ at module R . The resulting beam 3_2 is then passed into beam splitter B^2 , where it interferes with 2_2 , with subsequent detection at detectors 2_3 and 3_3 .

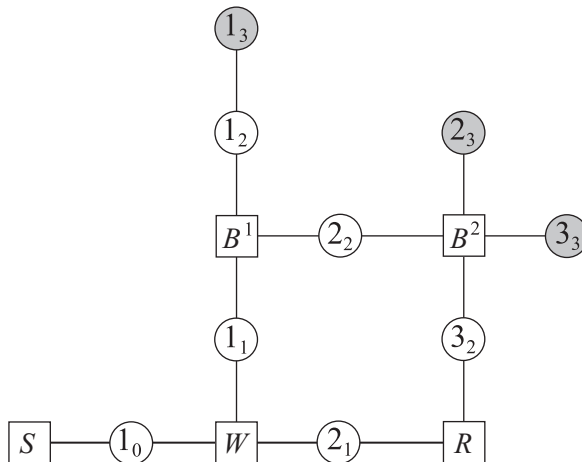


Figure 13.2. Brandt's network: source S prepares an unpolarized, monochromatic beam of light that passes through Wollaston prism W . This splits the beam into two orthogonally polarized components. These are passed through beam splitters B^1 and B^2 as shown. Module R rotates the polarization of one of the polarized beams into that of the other, prior to it being passed through B^2 .

Brandt's analysis was in terms of nonorthogonal system under observation (SUO) state vectors. Our analysis avoids nonorthogonality issues directly. The initial state is given by

$$|\Psi_0\rangle \equiv (\alpha|s_0^1\rangle + \beta|s_0^2\rangle) \otimes \widehat{\mathbb{A}}_0^1 \mathbf{0}_0 = (\alpha|s_0^1\rangle + \beta|s_0^2\rangle) \otimes \mathbf{1}_0, \tag{13.5}$$

where $|s_0^1\rangle, |s_0^2\rangle$ denote orthogonal photon polarization states, and α and β are complex coefficients satisfying $|\alpha|^2 + |\beta|^2 = 1$. By inspection of Figure 13.2 we take $N = 3, r_0 = 1, r_1 = 2, r_2 = r_3 = 3, d_0 = d_1 = d_2 = d_3 = 2$. The dynamics is given by the following rules.

Stage Σ_0 to Stage Σ_1

$$\begin{aligned} U_{1,0} \left\{ |s_0^1\rangle \otimes \widehat{\mathbb{A}}_0^1 \mathbf{0}_0 \right\} &\equiv |s_1^1\rangle \otimes \widehat{\mathbb{A}}_1^1 \mathbf{0}_1 = |s_1^1\rangle \otimes \mathbf{1}_1, \\ U_{1,0} \left\{ |s_0^2\rangle \otimes \widehat{\mathbb{A}}_0^1 \mathbf{0}_0 \right\} &\equiv |s_1^2\rangle \otimes \widehat{\mathbb{A}}_1^1 \mathbf{0}_1 = |s_1^2\rangle \otimes \mathbf{2}_1. \end{aligned} \tag{13.6}$$

Stage Σ_1 to Stage Σ_2

$$\begin{aligned} U_{2,1} \left\{ |s_1^1\rangle \otimes \widehat{\mathbb{A}}_1^1 \mathbf{0}_1 \right\} &\equiv t^1 |s_2^1\rangle \otimes \widehat{\mathbb{A}}_2^1 \mathbf{0}_2 + ir^1 |s_2^2\rangle \otimes \widehat{\mathbb{A}}_2^2 \mathbf{0}_2 = |s_2^1\rangle \otimes \{t^1 \mathbf{1}_1 + ir^1 \mathbf{2}_2\}, \\ U_{2,1} \left\{ |s_1^2\rangle \otimes \widehat{\mathbb{A}}_1^1 \mathbf{0}_1 \right\} &\equiv -|s_2^1\rangle \otimes \widehat{\mathbb{A}}_2^3 \mathbf{0}_2 = -|s_2^1\rangle \otimes \mathbf{4}_2, \end{aligned} \tag{13.7}$$

where $(t^1)^2 + (r^1)^2 = 1$. The second equation in (13.7) represents a rotation of the photon polarization vector $|s_1^2\rangle$ by $-\frac{1}{2}\pi$ into $-|s_2^1\rangle$ as it passes through the module labeled R in Figure 13.2 (the sign change follows the convention used in Brandt (1999)).

Stage Σ_2 to Stage Σ_3

$$\begin{aligned} U_{3,2} \left\{ |s_2^1\rangle \otimes \widehat{\mathbb{A}}_2^2 \mathbf{0}_2 \right\} &\equiv |s_3^1\rangle \otimes \widehat{\mathbb{A}}_3^2 \mathbf{0}_3 = |s_3^1\rangle \otimes \mathbf{1}_3, \\ U_{3,2} \left\{ |s_2^1\rangle \otimes \widehat{\mathbb{A}}_2^2 \mathbf{0}_2 \right\} &\equiv t^2 |s_3^1\rangle \otimes \widehat{\mathbb{A}}_3^3 \mathbf{0}_3 + ir^2 |s_3^1\rangle \otimes \widehat{\mathbb{A}}_3^3 \mathbf{0}_3 \\ &= t^2 |s_3^1\rangle \otimes \mathbf{4}_3 + ir^2 |s_3^1\rangle \otimes \mathbf{2}_3, \\ U_{3,2} \left\{ |s_2^2\rangle \otimes \widehat{\mathbb{A}}_2^3 \mathbf{0}_2 \right\} &\equiv ir^2 |s_3^1\rangle \otimes \widehat{\mathbb{A}}_3^3 \mathbf{0}_3 + t^2 |s_3^1\rangle \otimes \widehat{\mathbb{A}}_3^3 \mathbf{0}_3 \\ &= ir^2 |s_3^1\rangle \otimes \mathbf{4}_3 + t^2 |s_3^1\rangle \otimes \mathbf{2}_3, \end{aligned} \tag{13.8}$$

where $(t^2)^2 + (r^2)^2 = 1$.

With this information transcribed into Section *A* of the CA program MAIN, we find the following nonzero outcome probabilities for the Brandt network:

$$\begin{aligned} \Pr(\widehat{\mathbb{A}}_3^1 \mathbf{0}_3 | \Psi_0) &= |\alpha|^2 (t^1)^2, \\ \Pr(\widehat{\mathbb{A}}_3^2 \mathbf{0}_3 | \Psi_0) &= |\alpha|^2 (r^1 r^2)^2 - (\alpha^* \beta + \alpha \beta^*) r^1 r^2 t^2 + |\beta|^2 (t^2)^2, \\ \Pr(\widehat{\mathbb{A}}_3^3 \mathbf{0}_3 | \Psi_0) &= |\alpha|^2 (r^1 t^2)^2 + (\alpha^* \beta + \alpha \beta^*) r^1 r^2 t^2 + |\beta|^2 (r^2)^2, \end{aligned} \tag{13.9}$$

assuming perfect efficiency and wave-train overlap. When the reflection and transmission coefficients are chosen as by Brandt (Brandt, 1999), these rates agree with his precisely.

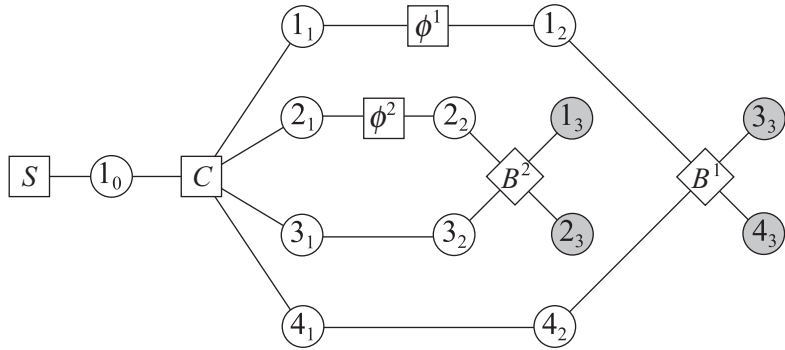


Figure 13.3. The HSZ two-photon interferometer.

13.4 The Two-Photon Interferometer

Up to now, we have restricted attention to signality-one processes. It is important to test our QDN approach on more subtle situations. With this in mind, in this section we discuss the application of QDN to a signality-two process discussed by Horne, Shimony, and Zeilinger (HSZ) (Horne et al., 1989). The relevant stage diagram is given in Figure 13.3.

A source S creates a preparation switch 1_0 that by stage Σ_1 has generated a two-photon entangled state via module C . As discussed in Horne et al. (1989), module C creates four separate components that are processed as follows. Component 1_1 passes through phase changer ϕ^1 and then enters beam splitter B^1 , while component 2_1 passes through phase changer ϕ^2 and then enters beam splitter B^2 . Components 3_1 and 4_1 pass directly on to beam splitters B^2 and B^1 , respectively, as shown. The observer monitors signals at stage Σ_3 as shown. The aim of the experiment is to investigate photon signal pair correlations in the detectors.

Parameters

We take $N = 3$, $d[0] = d[1] = d[2] = d[3] = 1$, $r[0] = 1$, $r[1] = r[2] = r[3] = 4$.

Initial State

The preparation switch is given by

$$|\Psi, 0\rangle = |s_0^1\rangle \otimes \widehat{A}_0^1 \mathbf{0}_0. \tag{13.10}$$

Evolution

Stage Σ_0 to Σ_1

$$U_{1,0} \left\{ |s_0^1\rangle \otimes \widehat{A}_0^1 \mathbf{0}_0 \right\} \equiv \frac{1}{\sqrt{2}} |s_1^1\rangle \otimes \left\{ \widehat{A}_1^1 \widehat{A}_1^3 \mathbf{0}_1 + \widehat{A}_1^2 \widehat{A}_1^4 \mathbf{0}_1 \right\} = \frac{1}{\sqrt{2}} |s_1^1\rangle \otimes \{ \mathbf{5}_1 + \mathbf{10}_1 \}. \tag{13.11}$$

Stage Σ_1 to Σ_2

$$U_{2,1} \left\{ |s_1^1\rangle \otimes \widehat{\mathbb{A}}_1^1 \widehat{\mathbb{A}}_1^3 \mathbf{0}_1 \right\} \equiv e^{i\phi^1} |s_2^1\rangle \otimes \widehat{\mathbb{A}}_2^1 \widehat{\mathbb{A}}_2^3 \mathbf{0}_2 = e^{i\phi^1} |s_2^1\rangle \otimes \mathbf{5}_2, \quad (13.12)$$

$$U_{2,1} \left\{ |s_1^1\rangle \otimes \widehat{\mathbb{A}}_1^2 \widehat{\mathbb{A}}_1^4 \mathbf{0}_1 \right\} \equiv e^{i\phi^2} |s_2^1\rangle \otimes \widehat{\mathbb{A}}_2^2 \widehat{\mathbb{A}}_2^4 \mathbf{0}_2 = e^{i\phi^2} |s_2^1\rangle \otimes \mathbf{10}_2. \quad (13.13)$$

Stage Σ_2 to Σ_3

$$\begin{aligned} U_{3,2} \left\{ |s_2^1\rangle \otimes \widehat{\mathbb{A}}_2^1 \widehat{\mathbb{A}}_2^3 \mathbf{0}_2 \right\} &= |s_3^1\rangle \otimes \left\{ t^1 \widehat{\mathbb{A}}_3^4 + ir^1 \widehat{\mathbb{A}}_3^3 \right\} \left\{ t^2 \widehat{\mathbb{A}}_3^1 + ir^2 \widehat{\mathbb{A}}_3^2 \right\} \\ &= |s_3^1\rangle \otimes \left\{ t^1 t^2 \mathbf{9}_3 + ir^1 t^2 \mathbf{5}_3 + ir^2 t^1 \mathbf{10}_3 - r^1 r^2 \mathbf{6}_3 \right\}, \\ U_{3,2} \left\{ |s_2^1\rangle \otimes \widehat{\mathbb{A}}_2^2 \widehat{\mathbb{A}}_2^4 \mathbf{0}_2 \right\} &= |s_3^1\rangle \otimes \left\{ t^2 \widehat{\mathbb{A}}_3^2 + ir^2 \widehat{\mathbb{A}}_3^1 \right\} \left\{ t^1 \widehat{\mathbb{A}}_3^3 + ir^1 \widehat{\mathbb{A}}_3^4 \right\} \\ &= |s_3^1\rangle \otimes \left\{ t^1 t^2 \mathbf{6}_3 + ir^2 t^1 \mathbf{5}_3 + ir^1 t^2 \mathbf{10}_3 - r^1 r^2 \mathbf{9}_3 \right\}. \end{aligned} \quad (13.14)$$

With this information, program MAIN gives the following nonzero correlation probabilities:

$$\begin{aligned} \Pr(\widehat{\mathbb{A}}_3^1 \widehat{\mathbb{A}}_3^3 \mathbf{0}_3 | \Psi_0) &= \Pr(\widehat{\mathbb{A}}_3^2 \widehat{\mathbb{A}}_3^4 \mathbf{0}_3 | \Psi_0) = \frac{1}{2}(r^1 t^2)^2 + \frac{1}{2}(r^2 t^1)^2 + r^1 r^2 t^1 t^2 \cos(\phi^1 - \phi^2), \\ \Pr(\widehat{\mathbb{A}}_3^2 \widehat{\mathbb{A}}_3^3 \mathbf{0}_3 | \Psi_0) &= \Pr(\widehat{\mathbb{A}}_3^1 \widehat{\mathbb{A}}_3^4 \mathbf{0}_3 | \Psi_0) = \frac{1}{2}(r^1 r^2)^2 + \frac{1}{2}(t^2 t^1)^2 - r^1 r^2 t^1 t^2 \cos(\phi^1 - \phi^2). \end{aligned} \quad (13.15)$$

These agree with the results given in Horne et al. (1989), assuming no losses and taking $t^1 = r^1 = t^2 = r^2 = 1/\sqrt{2}$.

The following comments are relevant.

Partial Questions

The above signal pair correlations show dependency on the phases ϕ^1, ϕ^2 , whereas as pointed out by HSZ, the answers to the partial questions involving single detectors only have no such dependence. For instance, the probability $\Pr(1_3 | \Psi_0)$ that stage Σ_3 detector 1₃ has fired is given by

$$\Pr(1_3 | \Psi_0) = \Pr(\widehat{\mathbb{A}}_3^1 \widehat{\mathbb{A}}_3^3 \mathbf{0}_3 | \Psi_0) + \Pr(\widehat{\mathbb{A}}_3^1 \widehat{\mathbb{A}}_3^4 \mathbf{0}_3 | \Psi_0) = \frac{1}{2}, \quad (13.16)$$

which is independent of the phases. The same result holds for the other single detectors.

Nonlocality

The QDN formalism shows that the phase change ϕ^1 applied to component 1₁ could be applied to component 3₁ instead with no change in physical predictions; this is evident from the fact that the phase factor $\exp(i\phi^1)$ multiplies the product $\widehat{\mathbb{A}}_2^1 \widehat{\mathbb{A}}_2^3$ in Eq. (13.12). A similar remark applies to the other phase change ϕ^2 . Since the component beams are spatially separated when this phase change is applied, this means that quantum states are inherently nonlocal in character.

From such considerations, we conclude that physical space is not as simple as it seems from a classical perspective. Perhaps a better way of saying this is that the classical model of physical space as a three-dimensional continuum of spatial position parameters is a good classical model but contextually incomplete as far as quantum mechanics is concerned.

Probabilities versus Rates

As with all calculations in QDN, normalization to unity is an idealization that avoids empirically significant but theoretically marginal considerations to do with flux factors, particle production rates, and such like. Perhaps the best way to deal with these issues is to recognize that what is calculated represents idealized situations. The more empirically useful interpretation of stated probabilities is that they are *best case rates*, that is, predicted relative average signal rates during the time when incoming wave trains are long enough to intersect and interfere, with no inefficiencies or extraneous losses in detection.